



Reprinted from JOURNAL OF THE ELECTROCHEMICAL SOCIETY  
Vol. 139, No. 12, December 1992  
Printed in U.S.A.  
Copyright 1992

# Scanning Electrochemical Microscopy 18

## Thin Layer Cell Formation with a Mercury Pool Substrate

Michael V. Mirkin and Allen J. Bard\*

Department of Chemistry and Biochemistry, The University of Texas at Austin, Austin, Texas 78712

### ABSTRACT

Scanning electrochemical microscopic (SECM) experiments were carried out with a liquid Hg substrate. Two types of responses were observed: (i) conventional steady-state positive feedback  $i$ - $d$  (current-distance) curves typical for SECM with a conductive substrate, *i.e.*, a tip current growing approximately exponentially with a decrease in  $d$  as the tip approached the Hg surface and (ii) steady-state tip current independent of  $d$  after the tip penetrated the surface. The latter behavior was attributed to a thin layer of electrolyte brought inside the mercury pool by the ultramicroelectrode tip. The thickness of this layer, estimated from thin layer cell theory, was from several hundreds of nanometers to a few microns. Electrochemical measurements inside such a layer (*e.g.*, steady-state voltammetry) yielded kinetic parameters for the heterogeneous reduction of  $\text{Ru}(\text{NH}_3)_6^{3+}$  at a carbon fiber in good agreement with those obtained from steady-state voltammograms at a microdisk electrode.

The scanning electrochemical microscope (SECM) has previously been employed in kinetic studies<sup>1-6</sup> and the chemical imaging<sup>1,7-11</sup> of various solid substrates, *e.g.*, metals, semiconductors, and ion-conductive polymers. In this paper we explore the possibility of SECM experiments with the electronically conductive liquid substrate Hg. A Hg substrate is interesting for several reasons: (i) an extremely close tip/substrate separation can be obtained and consequently the upper limit for the determinable rate constant can be extended, because the liquid substrate is essentially atomically smooth and horizontal, and the insulator surrounding the tip electrode can penetrate slightly into its volume without disturbing the measurements or destroying the tip. Rather complicated mercury pool and mercury-coated platinum electrode thin layer cells have been described,<sup>12</sup> but have not been widely used. (ii) Mercury is known to be a classic example of a smooth uniform electrode. It is also a very good substrate for studying adsorption and new phase formation phenomena. Moreover, experiments in this laboratory have shown that *in situ*

imaging of a Hg surface by scanning tunneling microscopy (STM) is difficult because of vibrations and tip interactions with the mercury surface.

We show here that SECM approach curves, *i.e.*, tip current ( $i_t$ ) vs. tip-Hg surface separation ( $d$ ), can be recorded. These agree well with the theoretical SECM response (positive feedback) expected for an electronically conductive substrate. After the tip penetrates the Hg surface, the SECM response reflected the formation of a thin layer of electrolyte trapped inside the mercury pool between the electrode tip and the Hg. Possible applications of the unique thin layer cell formed in this way, *e.g.*, in the examination of electrochemical kinetics, is discussed below.

### Experimental

**Materials.**—Triply distilled mercury (Bethlehem Apparatus Company Hellertown, Pennsylvania) was filtered before use. All other chemicals were reagent grade and were used without further purification. Millipore reagent water was used for the preparation of all aqueous solutions. Solutions were deoxygenated for at least 15 min with purified nitrogen before each experiment.

\* Electrochemical Society Active Member.

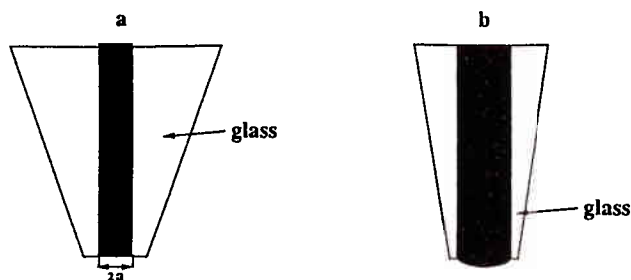


**Fig. 1.** Schematic representation of the two types of SECM tips used in this study. (a) A disk-shaped tip embedded in a conically ground insulating glass tube. The insulator radius was about two to three times the tip radius. (b) A tip shaped as a spherical segment slightly protruding from the insulating glass.

**Electrodes.**—Ultramicroelectrode (UME) tips were prepared by sealing 25  $\mu\text{m}$  diam platinum wire (Goodfellow Metals, Cambridge, England) or 11  $\mu\text{m}$  diam carbon fiber (Amoco Performance Products, Greenville, South Carolina) into glass as previously described.<sup>3,8</sup> The ends of the glass tubes surrounding the tips were ground into a conical shape. Two substantially different tip geometries were obtained by means of different grinding and polishing procedures. The first (type A) (Fig. 1a) was a conventional disk (either Pt or C) electrode surrounded by a thin insulating sheath (the total insulator diameter was only two to three times the electrode diameter) and was produced by sealing the wire in a glass capillary, tapering the end to reduce the diameter of the glass sheath, and then grinding flat. Although it is possible that this last grinding caused the Pt or C to be slightly recessed inside the glass sheath, microscopic examination did not reveal such a recession, and  $i_T$  vs.  $d$  curves with such electrodes over a solid substrate showed that the tip could approach to  $d/a$  levels (where  $a$  is the electrode radius) of less than 0.1 without a tip crash. In the second (type B) Pt tip (Fig. 1b) the Pt was a spherical segment that protruded by 1–5  $\mu\text{m}$  beyond the glass sheath, as seen by optical microscopy. This shape was attained by careful grinding. Before each experiment the microtip was polished with 0.05  $\mu\text{m}$  alumina on felt (Buehler Limited, Lake Bluff, Illinois). The substrate electrode, ~1 cm diam Hg pool, was placed in the bottom of a Teflon cell described previously.<sup>5</sup> The auxiliary electrode was a 0.5 mm diam Pt wire. A similar Pt wire immersed either into the solution or into the mercury pool (the last modification did not cause any change in response) served as a quasi-reference electrode (QRE).

**Apparatus.**—SECM measurements were performed using the instrument described previously.<sup>7</sup> The potential of the working electrode was controlled by a Princeton Applied Research (PAR) 175 universal programmer (Princeton, New Jersey). The voltammograms were obtained with a PAR 173 potentiostat. The SECM assembly rested on a vibration-free table (Newport Corporation, Fountain Valley, California) and was shielded in a Faraday cage. Failure to use vibration isolation techniques resulted in very noisy tip currents.

**SECM procedure.**—The SECM was used in a feedback mode as described previously.<sup>13</sup> The experiment was carried out with an aqueous solution containing 5 mM  $\text{Ru}(\text{NH}_3)_6^{3+}$  and 0.2M  $\text{KNO}_3$  as a supporting electrolyte. During the  $i_T$  vs.  $d$  scan, the tip was held at  $-0.5$  V vs. Pt quasi-reference electrode, where a steady-state plateau was obtained for the reduction of  $\text{Ru}(\text{NH}_3)_6^{3+}$  in the voltammogram, and the potential of unbiased substrate governed by redox species contained in the solution was sufficiently positive to oxidize  $\text{Ru}(\text{NH}_3)_6^{2+}$  generated at the tip back to  $\text{Ru}(\text{NH}_3)_6^{3+}$ . Alternatively, the same experiment could be performed with the Hg substrate purposely biased at a sufficiently positive potential (e.g., 0 V vs. Pt quasi-reference electrode). This modification led to essentially the same experi-

mental response. The tip current and position were recorded as the tip was scanned towards the substrate surface at speeds of 0.05–5  $\mu\text{m}/\text{s}$ . The  $i_T$ - $d$  curves were converted to absolute distance (where the zero-point corresponds to the Hg surface) by fitting the experimental data to theoretical diffusion-controlled SECM feedback curves.<sup>13,14</sup>

## Results and Discussion

**The SECM current-distance curves.**—Typical  $i_T$ - $d$  curves obtained with a type B 25  $\mu\text{m}$  diam Pt tip (ground as a spherical segment with height about 2  $\mu\text{m}$ , as shown in Fig. 1b) are shown in Fig. 2. The initial part of the  $i_T$ - $d$  curve in Fig. 2a displays an exponential-type growth of the tip current as the tip approaches the mercury pool. This part of the curve (Fig. 2b) corresponds to the known theory for SECM with a conductive substrate,<sup>13,14</sup> thus demonstrating the use of a Hg substrate for conventional SECM experiments. However, after the point of inflection at  $d \approx 0$ , where the tip penetrates the Hg, the slope of the  $i$ - $d$  curve decreased, and the tip current tended to a limiting value independent of distance. This limiting current was quite high (e.g., 17.6 times the steady-state tip current at a large distance from the substrate,  $i_{T,\infty}$ , in Fig. 2a). This suggests that rather than directly contacting the Hg, which would cause an immediate large increase in  $i_T$ , the tip traps a thin layer of the electrolyte between the tip and the Hg substrate electrodes whose limiting thickness is independent of  $d$ . This tip/electrolyte/substrate configuration behaves as a twin electrode thin layer cell (TLC) whose thickness,  $\ell$ , can be evaluated from the diffusion limiting current<sup>12</sup>

$$i_d = nFAc^* \frac{2D_o D_R}{(D_o + D_R)\ell} \quad [1]$$

where  $n$  is the number of electrons involved in electrode reaction,  $F$  is the Faraday constant,  $A$  is the tip electrode surface area ( $=\pi a^2$ , neglecting the small difference between the disk and spherical segment geometry),  $c^*$  is the bulk concentration of the electroactive species, and  $D_o$  and  $D_R$  are diffusion coefficients for the oxidized and reduced forms, respectively. Comparing Eq. 1 with the expression for the microdisk steady-state current in solution far from substrate

$$i_{T,\infty} = 4nFDc^*a \quad [2]$$

and assuming  $D_o = D_R$  one obtains

$$i_d/i_{T,\infty} = \pi a/(4\ell) \quad [3]$$

and  $\ell \approx 0.56$   $\mu\text{m}$ . The formation of this layer was completely reversible and a symmetrical  $i_T$ - $d$  curve was recorded when the tip scanning direction was reversed at some point after penetration (Fig. 2c). The shapes of the curves in Fig. 2a and c were fairly reproducible, but occasionally at some point the thin layer between the tip and the substrate collapsed, the tip touched the mercury, and the current increased by many orders of magnitude. When this occurred, the reverse scan of the tip away from the substrate displayed a large hysteresis apparently caused by a Hg meniscus attached to the tip.

The shape of  $i_T$ - $d$  curves for a spherically ground (type B) tip depended on the scanning velocity. At a slow speed of the tip approaching the substrate, the limiting current was somewhat lower, implying that the trapped liquid layer was thicker (Fig. 2d). Unlike the rather stable  $i_T$ -values usually obtained with solid substrates in SECM, with Hg the tip current was sensitive to vibrations, and very noisy  $i_T$ - $d$  curves were obtained without adequate vibration isolation (Fig. 2e).

The  $i_T$ - $d$  curves obtained with a disk-shaped (type A) 11  $\mu\text{m}$  diam carbon fiber tip (Fig. 3) showed essentially the same behavior, proving that the described effect is not completely governed by the tip material or shape. In this case, however, the different tip geometry led to a significantly lower limiting feedback current, i.e., a thicker trapped layer. From the data shown in Fig. 3 a value of  $\ell \approx 2.1$   $\mu\text{m}$  was found from Eq. 3. The  $i_T$ - $d$  curves were

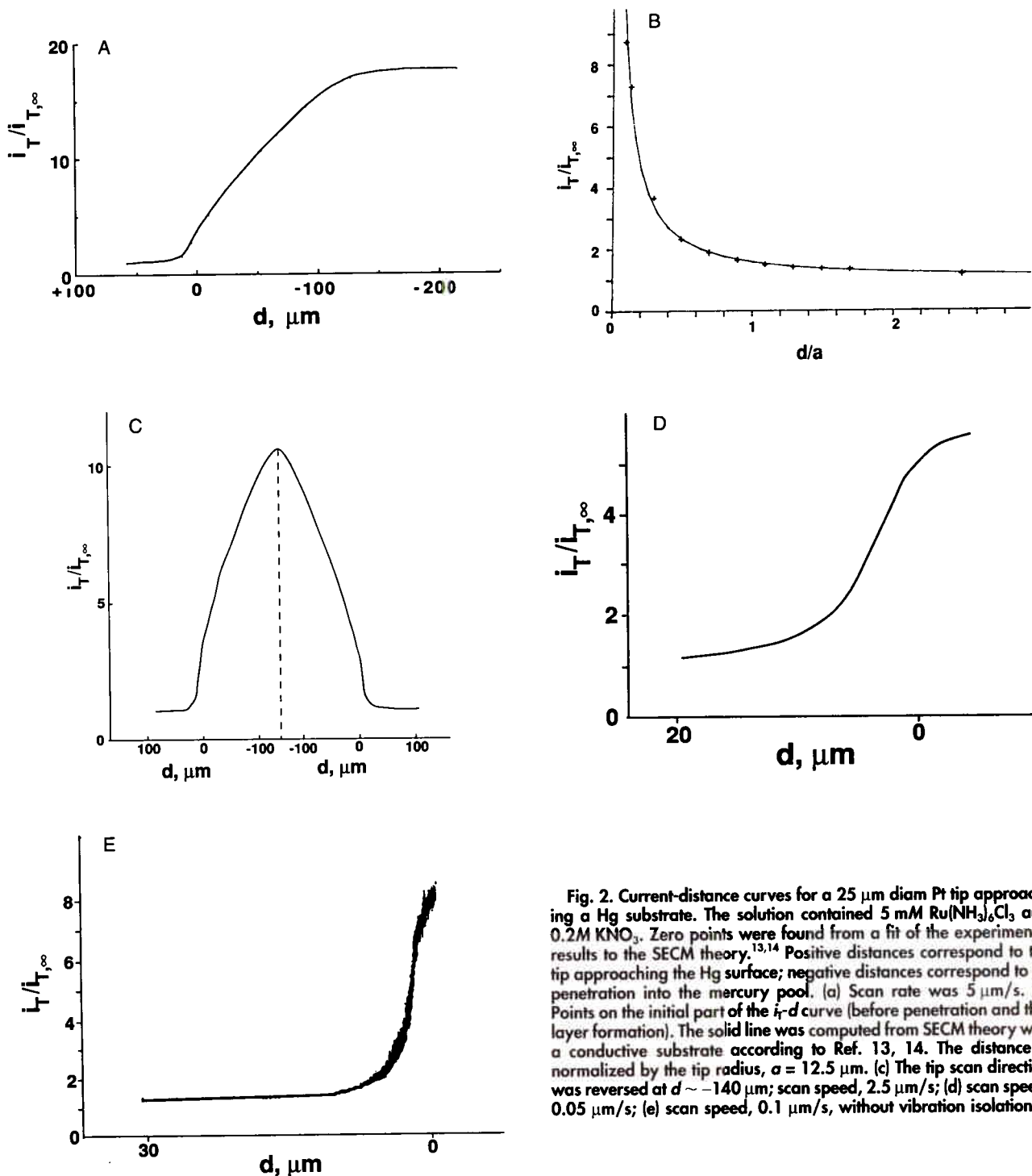


Fig. 2. Current-distance curves for a 25  $\mu\text{m}$  diam Pt tip approaching a Hg substrate. The solution contained 5 mM  $\text{Ru}(\text{NH}_3)_6\text{Cl}_3$  and 0.2M  $\text{KNO}_3$ . Zero points were found from a fit of the experimental results to the SECM theory.<sup>13,14</sup> Positive distances correspond to the tip approaching the Hg surface; negative distances correspond to tip penetration into the mercury pool. (a) Scan rate was 5  $\mu\text{m}/\text{s}$ . (b) Points on the initial part of the  $i_T$ - $d$  curve (before penetration and thin layer formation). The solid line was computed from SECM theory with a conductive substrate according to Ref. 13, 14. The distance is normalized by the tip radius,  $a = 12.5 \mu\text{m}$ . (c) The tip scan direction was reversed at  $d \sim -140 \mu\text{m}$ ; scan speed, 2.5  $\mu\text{m}/\text{s}$ ; (d) scan speed, 0.05  $\mu\text{m}/\text{s}$ ; (e) scan speed, 0.1  $\mu\text{m}/\text{s}$ , without vibration isolation.

highly reproducible, and their shape was virtually independent of approach (scanning) velocity. The trapped thin layer was quite stable; one could scan the tip back and forth laterally (*i.e.*, in the  $x$ - $y$  plane) over a distance of several microns without any effect on the layer thickness.

All the above findings suggest that the UME tip penetrating the mercury pool traps a layer of solution (a few micrometers in thickness) inside the pool. The mechanism by which this trapping occurs has not been investigated. It cannot involve only solvent and ions adsorbed on the tip and Hg, because only a few monolayers of electrolyte can be strongly attached to the electrode surface. A hydrodynamic picture of a rapidly advancing tip that does not give the solution sufficient time to leave the tip-substrate gap, is also not reasonable, especially for the disk-shaped tip, because in this case the shape of approach curves is independent of the scan rate. A better explanation is based on the

mercury surface responding to the pressure produced by the tip approaching the substrate (Fig. 4a). The resulting layer of liquid is then pushed by an advancing tip into the bulk of mercury and gets trapped there (Fig. 4b). Clearly, the rounded tip protruding from the insulating sheath (Fig. 1b) should drive a smaller amount of liquid into the mercury phase than a flat one (Fig. 1a) whose total surface area is larger. The fairly long distance (about 120  $\mu\text{m}$  in Fig. 2a) represents the tip travel from the point where the mercury bending just begins until a constant-thickness electrolyte layer is formed inside the pool. We do not have any additional information about how the thickness and shape of this layer changes as the tip penetrates the Hg. The tip and substrate electrodes apparently form a thin layer electrochemical cell. A quite small (submicron) layer thickness can be achieved in this way, thus providing opportunities for very fast electrochemical measurements.

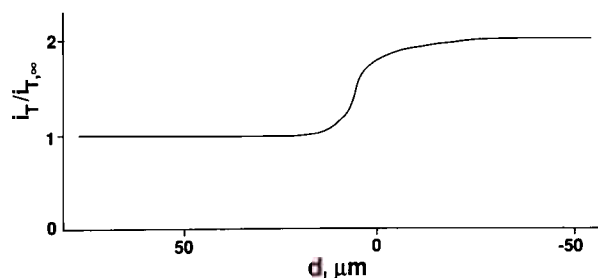


Fig. 3. The current-distance curve for an 11  $\mu\text{m}$  diam carbon tip approaching a Hg substrate; scan speed, 2.5  $\mu\text{m}/\text{s}$ . Electrolyte was the same as in Fig. 2.

Bindra *et al.*<sup>15</sup> have observed thin layer cell formation when a large carbon electrode (3 mm diam disk) was submerged in a mercury pool. The technique was used to grow droplets of Hg on a carbon electrode in a transient mode, but no thin layer steady-state measurements were reported.

**Cyclic voltammetry.**—The thin layer measurements inside the Hg pool are most useful when quantitative information can be extracted and the accuracy of the results demonstrated. Here we compare the kinetic parameters obtained for the quasi-reversible electroreduction of  $\text{Ru}(\text{NH}_3)_6^{3+}$  at a carbon fiber electrode obtained from the steady-state microdisk and thin layer cell voltammograms (Fig. 5a). Both types of voltammograms were analyzed by using a simple method we recently proposed,<sup>16</sup> which requires only knowledge of three experimental parameters, *i.e.*,  $E_{1/2}$ ,  $E_{1/4}$ , and  $E_{3/4}$  (the half-wave potential and two quartile potentials on the steady-state voltammogram), even when the formal potential,  $E^\circ$ , is unknown. From curve 1 in Fig. 5,  $|E_{1/4} - E_{1/2}| = 30.5$  mV and  $|E_{1/2} - E_{3/4}| = 33$  mV with an accuracy better than  $\pm 1$  mV. From these values and Table II in Ref. 16:  $E^\circ = E_{1/2} + 5$  mV =  $-319$  mV *vs.* QRE,  $\alpha = 0.40$  and  $\lambda = k^\circ a/D = 9.3$  (where  $k^\circ$  and  $\alpha$  are the standard heterogeneous rate constant and the transfer coefficient of the electrode reaction, respectively). Substituting into Eq. 2 the plateau current value,  $i_{T,\infty} = 6.6$  nA,  $c^* = 5$  mM and  $D = 6.3 \times 10^{-6}$  cm<sup>2</sup>/s,<sup>2</sup> we obtain  $a = 5.43$   $\mu\text{m}$  (in agreement with microscopic observation and the nominal diameter of the fiber) and  $k^\circ = \lambda D/a = 0.11$  cm/s.

Although the exact geometry of the above thin layer cell is unknown, one can still use the results of Ref. 15 as long as uniform accessibility of the tip surface can be assumed and an average mass-transfer coefficient,  $m$ , can be estimated. From the TLC current

$$m = i_d/nFAc^* = 0.031 \text{ cm/s} \quad [4]$$

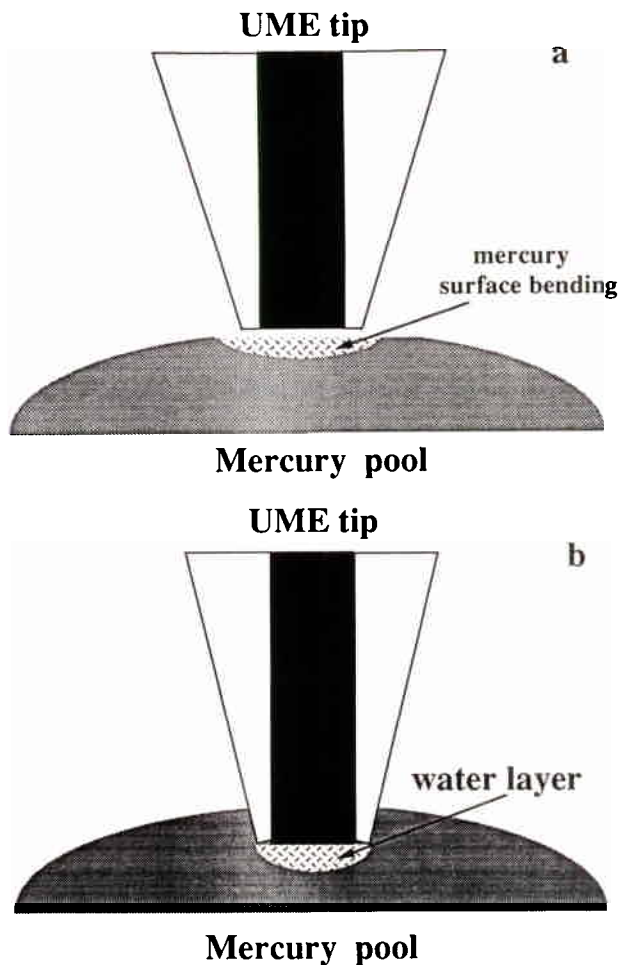
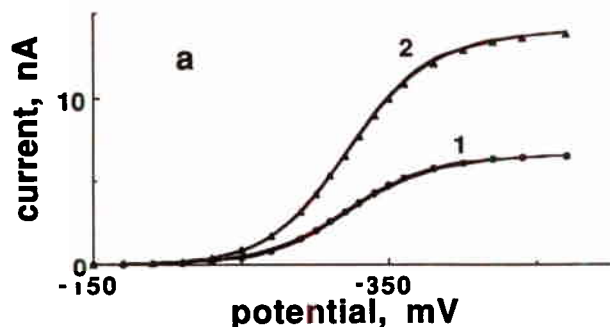


Fig. 4. Schematic representation of thin layer formation (a) and trapping (b) when the tip electrode penetrates the mercury pool. Note that the relative thickness of the trapped electrolyte layer to the UME diameter is exaggerated in this representation, *i.e.*, actual UME disk diameter/layer thicknesses are 25  $\mu\text{m}/0.56$   $\mu\text{m}$  and 11  $\mu\text{m}/2.1$   $\mu\text{m}$  for the Pt and C electrodes, respectively (see text).

With  $|E_{1/4} - E_{1/2}| = 30.5$  mV and  $|E_{1/2} - E_{3/4}| = 32.5$  mV (obtained from curve 2 in Fig. 5a) one can find from Table I in Ref. 16:  $E^\circ = E_{1/2} + 5$  mV =  $-318.5$  mV,  $\alpha = 0.44$  and  $\lambda = k^\circ/m = 5.0$ ; thus  $k^\circ = 0.15$  cm/s. The agreement between the parameters obtained from the steady-state long distance voltammogram and those found by this tip/Hg thin layer cell is very good, even with the high value of  $k^\circ$ , which is in

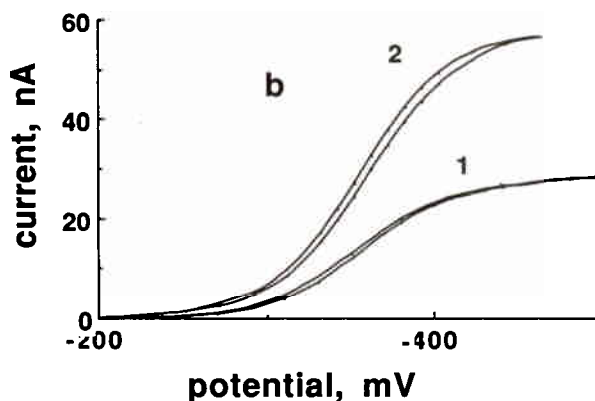


Fig. 5. Steady-state cyclic voltammograms of the solution containing 5 mM  $\text{Ru}(\text{NH}_3)_6\text{Cl}_3$  in 0.2M  $\text{KNO}_3$  at a carbon (a) and platinum (b) UME. 1, with the tip far from the substrate; 2, voltammograms obtained with tip within Hg, *i.e.*, in thin layer cell configuration. The potential scan rate was 5 mV/s (a) and 2 mV/s (b). Circles are calculated according to Eq. 13 in Ref. 17, and triangles according to Eq. 9 in Ref. 16 with the parameter values:  $k^\circ = 0.11$  cm/s,  $\alpha = 0.40$ ,  $E^\circ = -319$  mV (circles);  $k^\circ = 0.15$  cm/s,  $\alpha = 0.44$ ,  $E^\circ = -318.5$  mV (triangles).

fact close to the upper limit for measurements in this experiment. The theoretical curves calculated with these parameters also fit the experimental data. Note that the rate of a mass-transport in this thin layer cell is about twice as high as for the single microdisk electrode alone, where  $m \cong \pi D/2a \cong 0.018 \text{ cm/s}$ .<sup>16,17</sup>

The rate of the heterogeneous electron transfer reaction for reduction of  $\text{Ru}(\text{NH}_3)_6^{3+}$  is known to be much higher on Pt [ $k^\circ \sim 1 \text{ cm/s}$ ,<sup>18</sup>] so that analogous voltammograms of  $\text{Ru}(\text{NH}_3)_6^{3+}$  obtained with a Pt tip electrode (Fig. 5b) showed that this process is apparently Nernstian. A smaller tip would have to be used to obtain the kinetic parameters of this reaction on Pt.

### Conclusions

Electronically conductive (and possibly insulating) viscous liquids (*e.g.*, Hg) can serve as substrates in SECM experiments. A SECM tip shaped as a disk or a spherical segment penetrates the Hg surface and comes in with a micron-thick layer of electrolyte. Fast electrochemical measurements in such layers yield reliable values of kinetic parameters of heterogeneous electron transfer. The smallest thickness of this layer obtained thus far was about  $0.5 \mu\text{m}$  (with a  $25 \mu\text{m}$  diam tip electrode); smaller values of  $\ell$  probably can be obtained by using a smaller tip electrode.

### Acknowledgments

The support of this research by grants from the Texas Advanced Research Program and the National Science Foundation (CHE 8901450) is gratefully acknowledged.

Manuscript submitted April 13, 1992; revised manuscript received June 11, 1992.

The University of Texas at Austin assisted in meeting the publication costs of this article.

### REFERENCES

1. A. J. Bard, F.-R. F. Fan, D. T. Pierce, P. R. Unwin, D. O. Wipf, and F. Zhou, *Science*, **254**, 68 (1991), and references therein.
2. A. J. Bard, M. V. Mirkin, P. R. Unwin, and D. O. Wipf, *J. Phys. Chem.*, **96**, 1861 (1992).
3. D. O. Wipf and A. J. Bard, *This Journal*, **138**, 496 (1991).
4. M. V. Mirkin, F.-R. F. Fan, and A. J. Bard, *Science*, **257**, 364 (1992).
5. P. R. Unwin and A. J. Bard, *J. Phys. Chem.*, **95**, 7814 (1991).
6. R. C. Engstrom, B. Small, and L. Kattan, *Anal. Chem.*, **64**, 241 (1992).
7. A. J. Bard, G. Denuault, C. Lee, D. Mandler, and D. O. Wipf, *Acc. Chem. Res.*, **23**, 257 (1990), and references therein.
8. J. Kwak and A. J. Bard, *Anal. Chem.*, **61**, 1794 (1989).
9. C. Lee and A. J. Bard, *ibid.*, **62**, 1906 (1990).
10. J. Kwak and F. C. Anson, *ibid.*, **64**, 250 (1992).
11. D. O. Wipf and A. J. Bard, *This Journal*, **138**, L4 (1991).
12. A. T. Hubbard and F. C. Anson in *Electroanalytical Chemistry*, A. J. Bard, Editor, Vol. 4, p. 129, Marcel Dekker, Inc., New York (1970).
13. J. Kwak and A. J. Bard, *Anal. Chem.*, **61**, 1221 (1989).
14. M. V. Mirkin, F.-R. F. Fan, and A. J. Bard, *J. Electroanal. Chem.*, **328**, 47 (1992).
15. P. Bindra, A. P. Brown, M. Fleischmann, and D. Pletcher, *ibid.*, **58**, 39 (1975).
16. M. V. Mirkin and A. J. Bard, *Anal. Chem.*, **64**, 2393 (1992).
17. K. B. Oldham and C. G. Zoski, *J. Electroanal. Chem.*, **256**, 11 (1988).
18. T. Iwasita, W. Schmickler, and J. W. Schultze, *Ber. Bunsenges. Phys. Chem.*, **89**, 138 (1985).